

Robustness of oscillatory α^2 dynamos in spherical wedges

E. Cole^{1,2}, A. Brandenburg^{2,3,4,5}, P. J. Käpylä^{6,1,2} and M. J. Käpylä^{7,6}

¹ Department of Physics, Gustaf Hällströmin katu 2a, PO Box 64, University of Helsinki, 00014 Helsinki, Finland
e-mail: lizmcole@gmail.com

² Nordita, KTH Royal Institute of Technology and Stockholm University, Roslagstullsbacken 23, 10691 Stockholm, Sweden

³ Department of Astronomy, AlbaNova University Center, Stockholm University, 10691 Stockholm, Sweden

⁴ JILA and Department of Astrophysical and Planetary Sciences, Box 440, University of Colorado, Boulder, CO 80303, USA

⁵ Laboratory for Atmospheric and Space Physics, 3665 Discovery Drive, Boulder, CO 80303, USA

⁶ ReSoLVE Centre of Excellence, Department of Computer Science, Aalto University, PO Box 15400, 00076 Aalto, Finland

⁷ Max-Planck-Institut für Sonnensystemforschung, Justus-von-Liebig-Weg 3, 37077 Göttingen, Germany

Received 20 January 2016 / Accepted 6 July 2016

ABSTRACT

Context. Large-scale dynamo simulations are sometimes confined to spherical wedge geometries by imposing artificial boundary conditions at high latitudes. This may lead to spatio-temporal behaviours that are not representative of those in full spherical shells.

Aims. We study the connection between spherical wedge and full spherical shell geometries using simple mean-field dynamos.

Methods. We solve the equations for one-dimensional time-dependent α^2 and $\alpha^2\Omega$ mean-field dynamos with only latitudinal extent to examine the effects of varying the polar angle θ_0 between the latitudinal boundaries and the poles in spherical coordinates.

Results. In the case of constant α and η_t profiles, we find oscillatory solutions only with the commonly used perfect conductor boundary condition in a wedge geometry, while for full spheres all boundary conditions produce stationary solutions, indicating that perfect conductor conditions lead to unphysical solutions in such a wedge setup. To search for configurations in which this problem can be alleviated we choose a profile of the turbulent magnetic diffusivity that decreases toward the poles, corresponding to high conductivity there. Oscillatory solutions are now achieved with models extending to the poles, but the magnetic field is strongly concentrated near the poles and the oscillation period is very long. By changing both the turbulent magnetic diffusivity and α profiles so that both effects are more concentrated toward the equator, we see oscillatory dynamos with equatorward drift, shorter cycles, and magnetic fields distributed over a wider range of latitudes. Those profiles thus remove the sensitive and unphysical dependence on θ_0 . When introducing radial shear, we again see oscillatory dynamos, and the direction of drift follows the Parker-Yoshimura rule.

Conclusions. A reduced α effect near the poles with a turbulent diffusivity concentrated toward the equator yields oscillatory dynamos with equatorward migration and reproduces best the solutions in spherical wedges. For weak shear, oscillatory solutions are obtained only for perfect conductor field conditions and negative shear. Oscillatory solutions become preferred at sufficiently strong shear. Recent three-dimensional dynamo simulations producing solar-like magnetic activity are expected to lie in this range.

Key words. turbulence – magnetohydrodynamics (MHD) – hydrodynamics

1. Introduction

The Sun's magnetic field is generally believed to be the result of a turbulent $\alpha\Omega$ dynamo in which differential rotation plays an important role. This is referred to as the Ω effect, and it has long been identified as a robust mechanism for amplifying the azimuthal magnetic field of the Sun by winding up the poloidal field (Babcock 1961; Ulrich & Boyden 2005; Brown et al. 2010). The production of poloidal field, on the other hand, is more complicated and harder to verify in computer simulations, but it is thought to be associated with helical motions in the rotating, density stratified convection zone (Parker 1955; Steenbeck et al. 1966). This process is commonly parametrised by an α effect. Although there remain substantial uncertainties regarding the α effect as an important ingredient at large magnetic Reynolds numbers (Cattaneo & Hughes 2006), simulations of turbulence and rotating convection have subsequently confirmed that conventional estimates of α and turbulent diffusivity η_t are reasonably accurate up to moderate values of the magnetic Reynolds number (Sur et al. 2008; Käpylä et al. 2009).

Simulations also demonstrate the generation of differential rotation from anisotropic rotating convection, which amounts to

a relative value of 20–30% in latitude (e.g. Miesch et al. 2000; Käpylä et al. 2011). However, whether or not this is enough to drive an $\alpha\Omega$ dynamo as opposed to an α^2 dynamo, in which the Ω effect would be subdominant, can only be decided on the basis of quantitative calculations. Furthermore, in reality, α and η_t are tensors and additional mean-field effects such as turbulent pumping and $\Omega \times J$ effect are likely to contribute to dynamo solutions in stars (e.g. Rädler 1980; Warnecke et al. 2016).

In the absence of a conclusive answer, one tends to resort to qualitative arguments. One is related to the clear east-west orientation of bipolar regions in the Sun, which suggests that the azimuthal field must be much stronger than the poloidal field. Another argument is that $\alpha\Omega$ dynamos are usually cyclic and can display equatorward migration of magnetic field either through suitable radial differential rotation (Parker 1955; Steenbeck & Krause 1969a) or through sufficiently strong meridional circulation in the presence of an α effect that operates only in the surface layers (Choudhuri et al. 1995). However, both arguments are problematic. Although it is probably true that the azimuthal field is stronger than the poloidal, their ratio may not be large enough to justify the dominance of the Ω effect. Furthermore, α^2 dynamos may well be oscillatory

(e.g. Käpylä et al. 2013a; Masada & Sano 2014) and can display equatorward migration under suitable conditions (Mitra et al. 2010). A completely different argument that motivates the study of oscillatory α^2 dynamos are recent simulations of convective dynamos in spherical wedges and full shells that also show equatorward migration (Käpylä et al. 2012, 2013b; Warnecke et al. 2013; Augustson et al. 2015). It is now believed that the equatorward migration in the simulations is facilitated by a region of negative shear and positive (negative) α effect in the northern (southern) hemisphere – in accordance with the Parker-Yoshimura rule (Warnecke et al. 2014). Recently an alternative scenario was reported by Duarte et al. (2016), who found that the sign of the α effect can be inverted in certain parameter ranges allowing equatorward migration also with positive radial shear. Although it is unclear to what extent those simulations represent stellar magnetic fields, it might be helpful to understand first the mechanism operating in those simulations before trying to understand real stars.

The idea of simulating solar or stellar magnetic fields in spherical wedge-shaped geometries with perfectly conducting latitudinal boundaries goes back to an early paper by Jennings et al. (1990). These authors found that such solutions give a faithful representation of systems in full spherical shells. However, they only considered $\alpha\Omega$ dynamos. There are now concerns that this conclusion might not carry over to α^2 dynamos. Indeed, while the explanation of equatorward migration through α^2 dynamo action might work in spherical wedge simulations, there is the problem that such solutions have never been seen in full-shell simulations that extend not just to high latitudes, but go all the way to the poles. Indeed, α^2 dynamos in full spherical shells are known to be steady (Steenbeck & Krause 1969b). Exceptions are dynamos with an anisotropic α tensor (Rüdiger et al. 2003) and the non-axisymmetric oscillatory solutions found by Jiang & Wang (2006), but for an isotropic α effect, oscillatory axisymmetric α^2 dynamos seem to be an artefact of having imposed a boundary condition at high latitudes. One could choose another boundary condition; a normal-field (pseudo-vacuum) boundary condition might be an obvious choice, but from corresponding Cartesian simulations we know that this would again lead to oscillatory solutions, but with poleward migration (Brandenburg et al. 2009).

Although the mean-field description of oscillatory α^2 dynamos seems to face an internal inconsistency regarding the limit to full spherical shells, there remains the question whether certain plausible changes in the setup of the full spherical shell model could lead to oscillatory solutions that are internally consistent and otherwise similar to the solutions in spherical wedges. There is a priori no physical motivation for this, but from a mathematical point of view, this is a natural choice when trying to reproduce the conditions encountered previously with a perfect conductor boundary condition. One possibility is a suitable latitudinal η_t profile with a larger conductivity (weaker magnetic diffusion) at high latitudes to simulate the behaviour of perfect conductor boundary conditions used in spherical wedges.

In each of those cases, it is important to assess how much shear would be needed to change the dynamo mode into an $\alpha\Omega$ type mode. To keep things simple, we employ a one-dimensional model with only latitudinal extent. However, in its standard formulation, with radial derivatives simply being dropped, the first excited mode of such an $\alpha\Omega$ dynamo is non-oscillatory (Jennings et al. 1990). This is an artefact that is easily removed by substituting radial derivatives with a damping term (Kuzanyan & Sokoloff 1995; Moss et al. 2004), instead of setting them to zero.

We begin by describing our model in detail, next, we focus on the analysis of spherical wedges of different extent and turn then to full spherical shells with variable latitudinal η_t profiles. In view of the aforementioned complications regarding the possibility of oscillatory behaviour in the corresponding $\alpha\Omega$ dynamos, we also discuss the sensitivity of our solutions with respect to an additional damping term that mimics the otherwise neglected radial derivative terms.

2. Model

We consider the mean-field dynamo equation for the mean magnetic field $\bar{\mathbf{B}}$ with a given mean electromotive force $\bar{\mathcal{E}}$ in the form

$$\frac{\partial \bar{\mathbf{B}}}{\partial t} = \nabla \times (\bar{\mathbf{U}} \times \bar{\mathbf{B}} + \bar{\mathcal{E}} - \eta \mu_0 \bar{\mathbf{J}}), \quad (1)$$

where $\bar{\mathbf{U}} = \hat{\phi} \varpi \Omega$ is the mean flow from angular velocity with $\varpi = r \sin \theta$ being the distance from the axis, $\Omega(r, \theta)$ is the internal angular velocity, $\hat{\phi}$ is the unit vector in the azimuthal direction, $\bar{\mathbf{J}} = \nabla \times \bar{\mathbf{B}} / \mu_0$ is the mean current density, μ_0 is the vacuum permeability, and η is the non-turbulent magnetic diffusion coefficient. In the absence of a memory effect, and under the assumption of isotropic α effect and turbulent magnetic diffusivity η_t , the mean electromotive force is given by

$$\bar{\mathcal{E}} = \alpha \bar{\mathbf{B}} - \eta_t \mu_0 \bar{\mathbf{J}}. \quad (2)$$

We solve Eqs. (1) and (2) numerically using sixth-order finite differences in space and a third-order accurate time-stepping scheme. We employ the PENCIL CODE¹, which solves the governing equations in terms of the mean magnetic vector potential $\bar{\mathbf{A}}$, such that $\bar{\mathbf{B}} = \nabla \times \bar{\mathbf{A}}$. It is convenient to use the advective gauge (Brandenburg et al. 1995; Candelaresi et al. 2011), in which the electrostatic potential has a contribution $\bar{U}_\phi \bar{A}_\phi$, so that

$$\frac{\partial \bar{\mathbf{A}}}{\partial t} = -\varpi \bar{A}_\phi \nabla \Omega + \bar{\mathcal{E}} - \eta \mu_0 \bar{\mathbf{J}}. \quad (3)$$

To allow for the use of a one-dimensional model with $\bar{\mathbf{B}} = \bar{\mathbf{B}}(\theta, t)$, we restrict ourselves to an angular velocity profile that varies linearly in r , specifically, $\Omega(r, \theta) = r S(\theta)$, so the angular velocity gradient becomes $\nabla \Omega = (S, \partial_\theta S, 0)$. The mean current density is then

$$\bar{\mathbf{J}} = \mu_0^{-1} R^{-2} (D_\theta \bar{A}_\theta - D_\theta \partial_\theta \bar{A}_r, \partial_\theta \bar{A}_r, -\partial_\theta D_\theta \bar{A}_\phi), \quad (4)$$

where $D_\theta = \cot \theta + \partial_\theta$ is a modified θ derivative. To account for the neglect of r derivatives, we add in Eq. (3) a damping term of the form $-\mu^2 \bar{\mathbf{A}}$, that is, we have

$$\frac{\partial \bar{\mathbf{A}}}{\partial t} = -\varpi \bar{A}_\phi \nabla \Omega + \bar{\mathcal{E}} - \eta \mu_0 \bar{\mathbf{J}} - \mu^2 \bar{\mathbf{A}} \quad (\text{with } \partial_r = 0); \quad (5)$$

see Moss et al. (2004) for a survey of solutions for different values of μ . For α and η_t we use latitudinal profile functions of the form

$$\alpha = \alpha_0 \cos \theta (a_0 + a_2 \sin^2 \theta + \dots + a_n \sin^n \theta), \quad (6)$$

$$\eta_t = \eta_0 (e_0 + e_2 \sin^2 \theta + \dots + e_n \sin^n \theta), \quad (7)$$

¹ <http://pencil-code.github.com/>

where a_i and e_i are coefficients denoted by the vectors $\mathbf{a} = (a_0, a_2, a_4, \dots, a_n)$ and $\mathbf{e} = (e_0, e_2, e_4, \dots, e_n)$, respectively. However, we often refer to only the three first components as $\mathbf{a} = (a_0, a_2, a_4)$ and $\mathbf{e} = (e_0, e_2, e_4)$. These expansions can also be expressed in terms of Legendre polynomials, which are orthonormal functions that obey regularity at the poles. The occurrence of higher order terms in α has been associated with higher orders terms in $\mathbf{g} \cdot \boldsymbol{\Omega}$, which are normally omitted in theoretical calculations (Rüdiger & Brandenburg 1995).

As usual, the problem is governed by two dynamo numbers,

$$C_\alpha = \alpha_0 R / \eta_{t0}, \quad C_\Omega = S_0 R^2 / \eta_{t0}, \quad (8)$$

where $S(\theta) = S_0$ is now a constant. We consider the following sets of boundary conditions:

$$\bar{A}_\theta \bar{A}_r = \bar{A}_\theta = \bar{A}_\phi = 0 \quad (\text{SAA}; \text{regularity on } \theta = \theta_0), \quad (9)$$

$$\bar{A}_r = \partial_\theta \bar{A}_\theta = \bar{A}_\phi = 0 \quad (\text{ASA}; \text{perf. cond. on } \theta = \theta_0), \quad (10)$$

$$\partial_\theta \bar{A}_r = \bar{A}_\theta = \partial_\theta \bar{A}_\phi = 0 \quad (\text{SAS}; \text{normal field on } \theta = \theta_0), \quad (11)$$

where the sequence of letters S and A refer respectively to symmetric ($\partial_\theta = 0$) and antisymmetric (vanishing function value) of \bar{A}_r , \bar{A}_θ , and \bar{A}_ϕ across the boundary. The same conditions are also applied on the corresponding boundary in the southern hemisphere where $\pi - \theta = \theta_0$. In this work, no symmetry condition on the equator is applied, so the parity of the solution is not constrained.

As initial conditions, we assume a seed magnetic field consisting of low-amplitude Gaussian noise. Such a field is sufficiently complex so that the fastest growing eigenmode of either parity tends to emerge after a short time. We note that mixed parity solutions are only possible in the nonlinear regime (Brandenburg et al. 1989), but this will not be considered here. In this work, we adjust the values of C_α and C_Ω such that the solutions are marginally excited, in other words, the field neither grows nor decays.

3. Results

We consider separately the cases where the dynamo is driven either solely by the α effect (α^2 dynamos) or by the combined action of the α effect and large-scale shear ($\alpha^2\Omega$ dynamos).

3.1. α^2 dynamos

3.1.1. Varying θ_0

We begin by considering the simplest case with $\mathbf{a} = (1, 0, 0)$ and $\mathbf{e} = (1, 0, 0)$, resulting in a spatially constant turbulent diffusivity and a $\cos \theta$ profile for α . We have calculated the critical value of C_α , hereafter C_α^* , for an α^2 dynamo where $C_\Omega = 0$. We used the boundary conditions SAA, ASA, and SAS for selected values of θ_0 .

It turns out that C_α^* decreases as we approach the pole ($\theta_0 \rightarrow 0^\circ$); see Fig. 1. The SAA and SAS boundary conditions result in very similar non-oscillatory solutions with a C_α^* of only approximately 40% of that C_α^* obtained for the ASA boundary condition. Oscillatory solutions show travelling waves that propagate equatorward; see Fig. 2. The boundary condition with the greatest variation of C_α^* with θ_0 is the perfect conductor, ASA. We also find that the most easily excited dynamo mode changes from stationary to oscillatory as θ_0 increases from zero to one degree in that case. For the case where $\theta_0 = 1^\circ$ we find both stationary and oscillatory solutions, depending on the initial conditions.

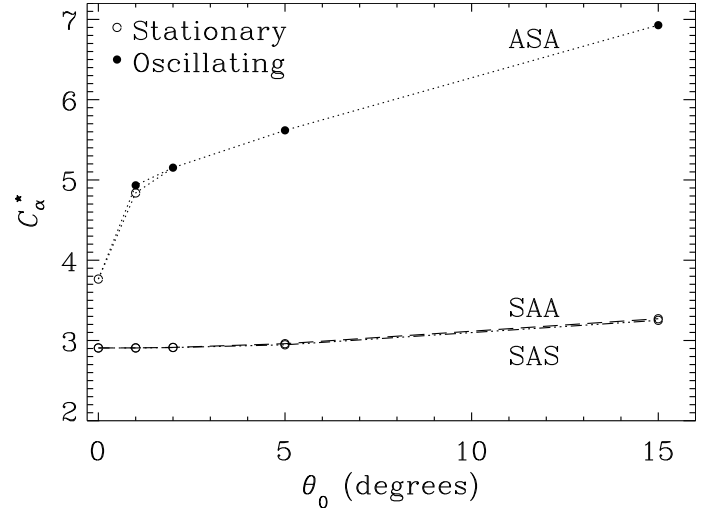


Fig. 1. Dependence of C_α^* on θ_0 for the three boundary conditions ASA, SAA, and SAS.

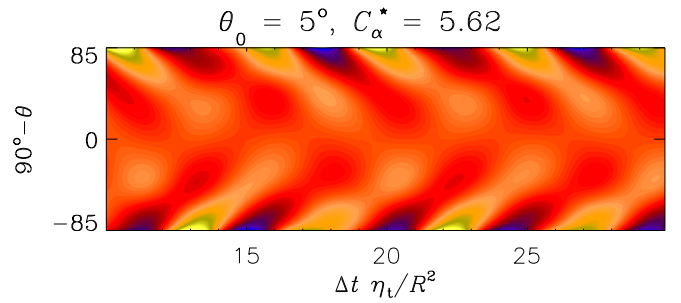


Fig. 2. Azimuthal magnetic field \bar{B}_ϕ for an oscillatory dynamo with $\theta_0 = 5^\circ$ and the boundary condition ASA.

The critical dynamo number is slightly higher for the oscillatory mode than for the corresponding stationary solution.

These results suggest that we cannot regard the limit $\theta_0 \rightarrow 0^\circ$ with the isotropic α effect and turbulent diffusivity using perfect conductor boundaries as an approximation to the full spherical shell model when searching for oscillatory solutions. Thus, the limit $\theta_0 \rightarrow 0^\circ$ is singular in this sense. Extending the model to the poles with the ASA boundary condition changes the resulting dynamo from oscillatory to stationary. The SAA and SAS boundary conditions give stationary solutions with relatively similar values for C_α^* , but the ASA boundary condition near the poles gives both oscillatory and stationary solutions, depending on the initial conditions of the seed magnetic field. While no stationary solutions were found for $\theta_0 > 1^\circ$, their existence is not ruled out by our models.

3.1.2. Varying latitudinal η_t profile

Given that we have found the limit $\theta_0 \rightarrow 0^\circ$ in the case of the perfect conductor boundary condition not to be an approximation to a full spherical shell model, we now investigate whether physically motivated alterations of the full spherical shell model with the SAA boundary condition could produce oscillatory, equatorward solutions similar to those found for $\theta_0 \neq 0^\circ$ with the ASA boundary condition. An obvious possibility is the use of an η_t profile that corresponds to high conductivity near the pole. Such a profile could correspond to the possible effect of rotation

Table 1. C_α^* for pure α^2 dynamos with varied magnetic diffusivity and α profiles and the corresponding oscillations frequencies in units of η_{t0}/R^2 .

	α		
	(1, 0, 0)	(0, 1, 0)	(0, 0, 1)
e_n	$C_\alpha^* \omega$	$C_\alpha^* \omega$	$C_\alpha^* \omega$
e_2	0.236 –	4.063 0.405	9.532 0.562
e_2	0.558 –	5.308 0.288	11.39 0.654
e_4	0.096 0.008	1.045 0.207	4.144 0.298
e_4	0.326 –	2.587 0.332	7.039 0.548
e_6	0.070 0.005	0.541 0.184	2.175 0.215
e_6	0.265 –	1.733 0.258	4.857 0.419
e_8	0.059 0.003	0.403 0.131	1.463 0.165
e_8	0.238 –	1.384 0.199	3.727 0.364

on the magnetic diffusivity (Kitchatinov et al. 1994) at various latitudes.

One possible alteration to the diffusivity profile is to use higher order terms for η_t . In particular, we examine solutions where the orders $n = 2, 4, 6$, and 8 are used for e_n ; see Eq. (7). Solutions are examined for $e_0 = \eta/\eta_{t0} = 0.01$ and 0.05. A non-zero uniform value of η is needed to ensure the stability of the solutions in the cases where the turbulent magnetic diffusivity is zero at the poles due to the profiles being proportional to powers of $\sin\theta$, which vanishes at the poles. We have verified that neither value of η used here leads to spurious growth in the absence of an α -effect. Furthermore, we calculate the oscillation frequency as $\omega = 2\pi/T$ where T is the period of oscillation for the large-scale magnetic field.

Values for C_α^* are indicated in Table 1 for cases where the turbulent diffusivity and α effect profiles are expanded up to orders e_8 and e_4 , respectively. We find that for $\alpha = (1, 0, 0)$, the $e_0 = 0.05$ case produces only stationary solutions, but at $e_0 = 0.01$, only solutions for $n = 2$ are stationary and all higher orders oscillate; see Table 1. Some solutions initially show rapidly oscillating behaviour, exhibiting antisymmetry with respect to the equator, but these disappear later and only a slower, persistent oscillatory mode remains; see Fig. 3a. These low-frequency oscillations have neither equatorward nor poleward migration and are symmetric about the equator. C_α^* increases with e_0 , and decreases as n increases for e_n , in accordance with the total diffusivity increasing and decreasing, respectively. The frequency of the oscillatory modes found for $e_0 = 0.01$ decreases as n increases. This is also consistent with mean-field theory where the oscillation frequency is proportional to the magnetic diffusion coefficient. The magnetic field is antisymmetric with respect to the equator in all cases, except for $\alpha = (1, 0, 0)$ and $e_0 = 0.01$; see Fig. 3a.

The azimuthal magnetic field is strongly concentrated toward the poles when the α effect has only the $\cos\theta$ variation in latitude; see the top panels of Figs. 3 and 4. In view of the equatorial magnetic field concentration in the Sun and in three-dimensional solar dynamo simulations, where the kinetic helicity is known to be strongly concentrated toward the equator (Käpylä et al. 2012), it is of interest to consider models with $\alpha = (0, 1, 0)$ and $\alpha = (0, 0, 1)$, so that the α effect is more concentrated toward lower latitudes. Indications for α being stronger at lower latitudes have been observed, for example, in models of rapidly rotating convection (Käpylä et al. 2006). The values for C_α^* are given in Table 1, columns for $\alpha = (0, 1, 0)$ and $\alpha = (0, 0, 1)$. A

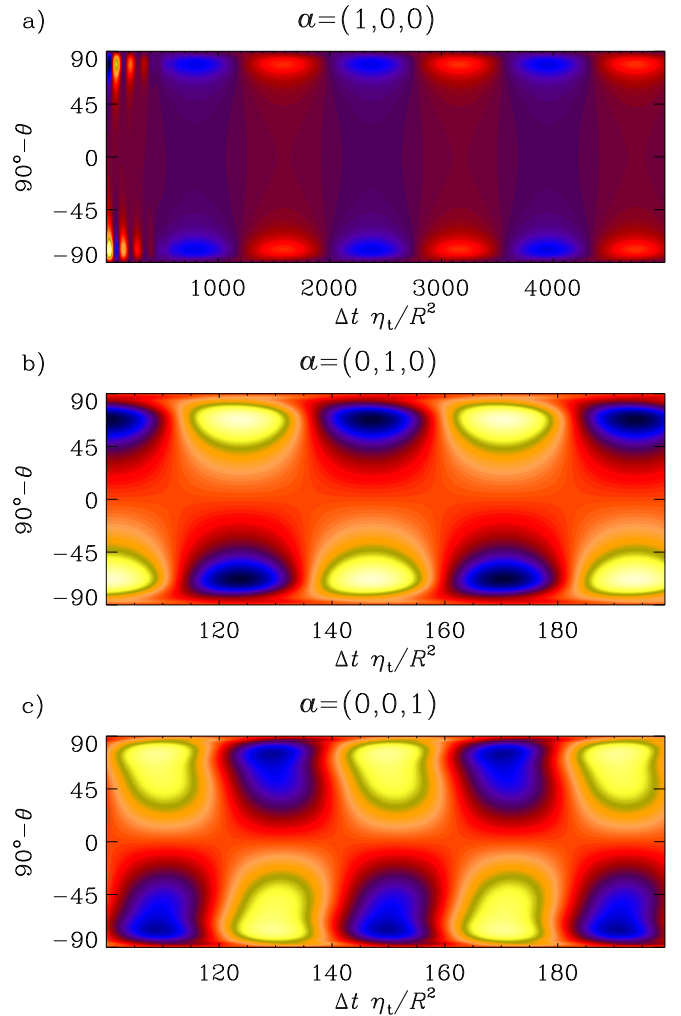


Fig. 3. Azimuthal magnetic field for $e_4, e_0 = 0.01$ in Table 1 with $\theta_0 = 0^\circ$ and the SAA condition.

similar trend as for the case where $\alpha = (1, 0, 0)$ is seen, where higher orders of e_n result in lower values for C_α^* , in accordance with lower total diffusion. Changes in the α profile have a larger effect on C_α^* than changes in the diffusivity profile. However, this is simply because, owing to the presence of the $\cos\theta$ factor in the α profile, its maximum value diminishes as higher powers of $\sin\theta$ are used, while the maximum value of η_t is always unity, irrespective of the profile. The oscillation frequencies of the solutions for $\alpha = (0, 1, 0)$ and $\alpha = (0, 0, 1)$ are two orders of magnitude higher than the low-frequency mode seen for $\alpha = (1, 0, 0)$. It turns out that the magnetic field is then more uniformly distributed over all latitudes; see Figs. 3 and 4. For $e_0 = 0.01$, this distribution is largely uniform with very slight equatorward drift (Figs. 3b and c), and when $e_0 = 0.05$, the equatorward drift becomes more pronounced and extends to lower latitudes (Figs. 4b and c).

In summary, extending the model all the way to the poles and including an η_t profile concentrated toward the equator results in oscillatory behaviour with long cycles but no equatorward migration. Including an α -effect also concentrated at lower latitudes produces equatorward cycles with shorter cycle periods with the strongest magnetic fields appearing at lower latitudes. These results are in qualitative agreement with direct and large-eddy simulations (Käpylä et al. 2012, 2013b; Augustson et al. 2015; Duarte et al. 2016).

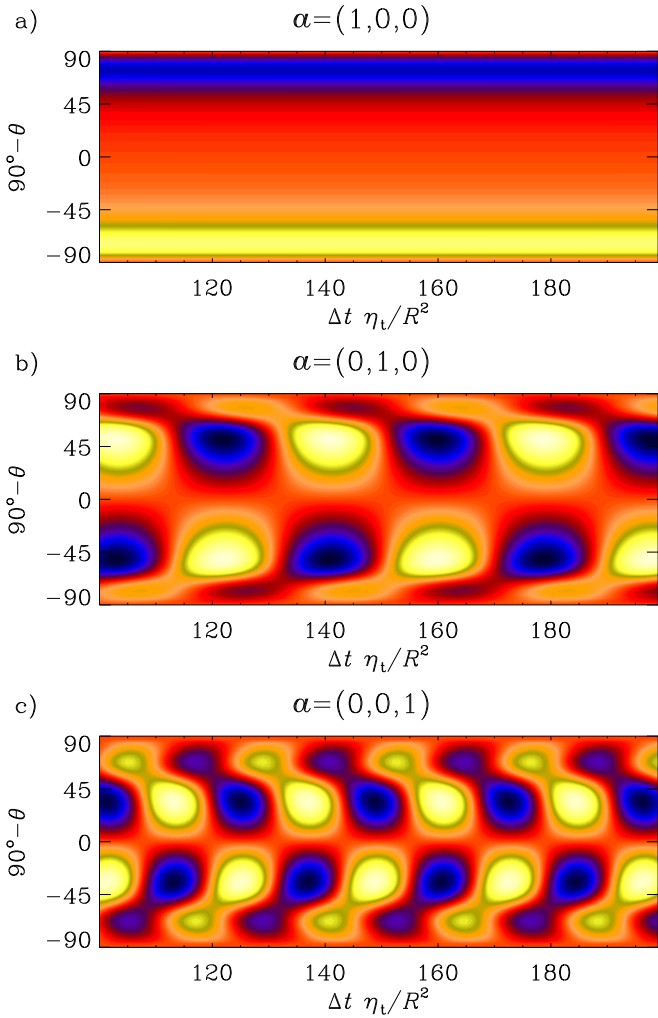


Fig. 4. Azimuthal magnetic field for $e_4, e_0 = 0.05$ in Table 1 with $\theta_0 = 0^\circ$ and the SAA condition.

We examine the impact of changing θ_0 on the resulting magnetic field using the same \boldsymbol{a} and \boldsymbol{e} in Fig. 4c. As θ_0 approaches zero, C_a^* changes in a continuous fashion both for the ASA and SAA boundary conditions; see Fig. 5. Thus, the limit $\theta_0 \rightarrow 0^\circ$ is now no longer singular. If the azimuthal fields are compared for the oscillatory solutions (Figs. 6 and 4c), solutions are equatorward and the only significant difference is that the ASA boundary condition produces fields strongest at the boundary, whereas the SAA boundary condition concentrates the field at lower latitudes.

3.2. $\alpha^2\Omega$ dynamos

Given that the commonly used ASA boundary condition was previously found to yield non-singular behaviour – even for a uniform η_t profile (Jennings et al. 1990), it is now of interest to re-address this problem in the context of the present model.

3.2.1. Overall behaviour of dynamo solutions

We now add large-scale radial shear and a damping term given by $\mu R^2/\eta_t$ and use $\tilde{\mu}$ to denote $\mu R^2/\eta_{t0}$. We first explore the dynamo regimes and the dependency on $\tilde{\mu}$ by setting $\theta_0 = 1^\circ$ and once again use $\boldsymbol{a} = (1, 0, 0)$ and $\boldsymbol{e} = (1, 0, 0)$. The critical value

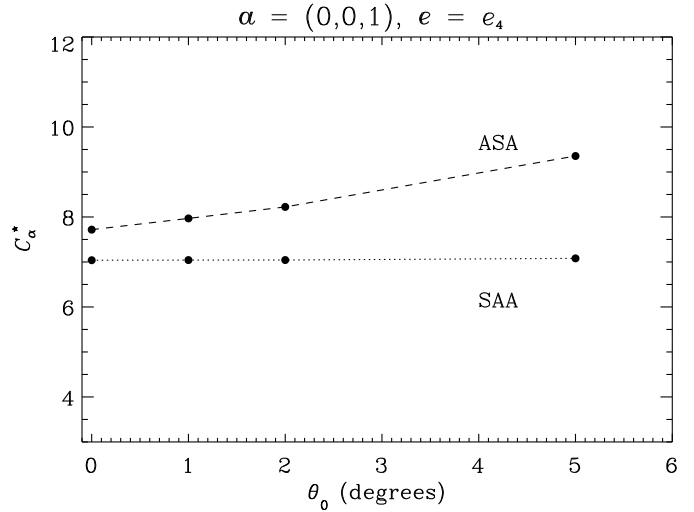


Fig. 5. Dependence of C_a^* on θ_0 for the ASA and SAA boundary conditions for $e_4, e_0 = 0.05$ and $\boldsymbol{a} = (0, 0, 1)$

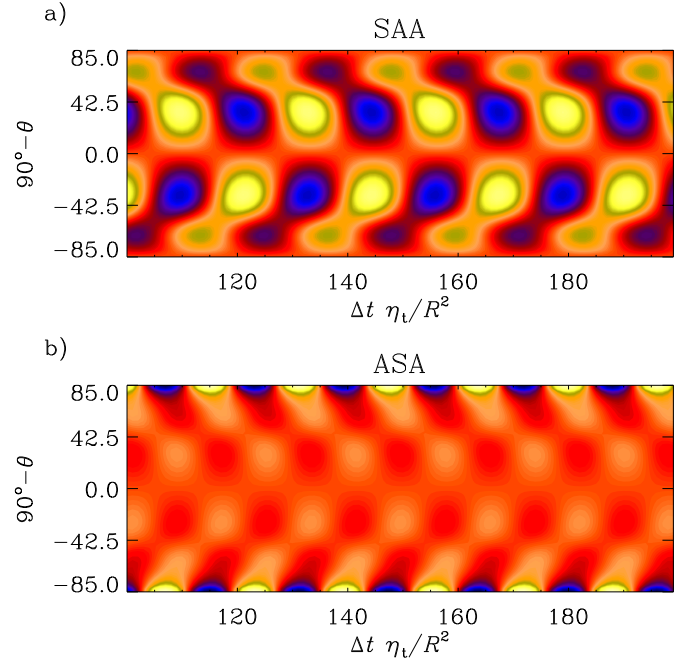


Fig. 6. Azimuthal magnetic field for $\theta_0 = 5^\circ$, $\boldsymbol{a} = (0, 0, 1)$, $e_4, e_0 = 0.05$, and the SAA (a) and ASA (b) boundary conditions.

C_a^* now depends on the value of $\tilde{\mu}$; see Fig. 7. We now concentrate on studying the dynamo modes that are excited in the system for values of $\tilde{\mu}$ between 0 and 4 and various values of C_Ω .

When $\tilde{\mu} = 0$, all resulting dynamos are stationary, with the exception of the case where $C_\Omega = 0$ where oscillations depend on initial conditions, and C_a^* decreases as C_Ω increases. For solutions pertaining to $\tilde{\mu} = 1$, two solutions exist in the regime $C_\Omega \gtrsim 33.5$ with either oscillatory or stationary magnetic fields. When C_Ω is less than this value, we find only stationary solutions. Near this limit, the frequency of oscillations is sensitive to both C_a^* and C_Ω and even small changes can double the frequency. The C_a^* for stationary dynamos is significantly less than for oscillating solutions. It is possible that for $\tilde{\mu} > 1$ a similar bifurcation also exists, as there always appears a change in the dependence of cycle frequency on C_a^* as the dynamo mode changes

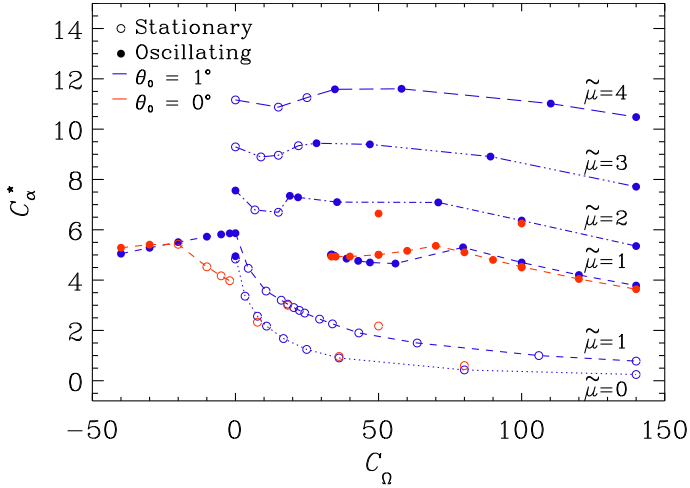


Fig. 7. Values for C_α^* as a function of C_Ω for oscillatory (filled circles) and stationary (open circles) solutions for $\theta_0 = 1^\circ$ (blue) and $\theta_0 = 0^\circ$ (red).

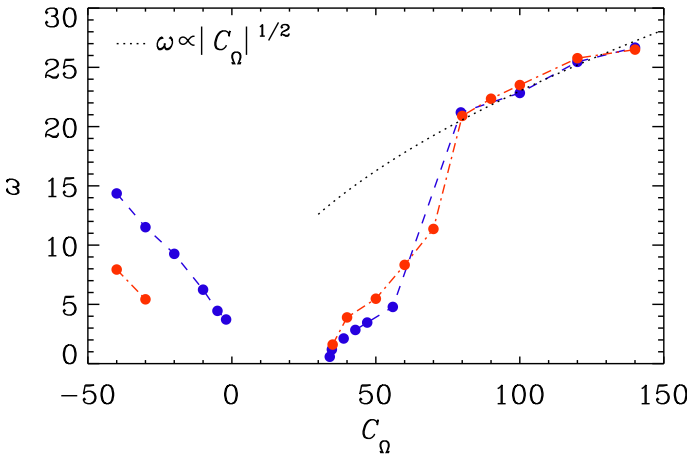


Fig. 8. Dependence of ω on C_Ω for $\theta_0 = 1^\circ$ (blue) and $\theta_0 = 0^\circ$ (red) for $\tilde{\mu} = 1$.

from stationary to oscillatory. However, at least in the case with $\tilde{\mu} = 2$, the stationary solutions were found to disappear. For cases where $\tilde{\mu} > 2$, C_α^* decreases with C_Ω , and oscillations only occur above certain critical values for C_Ω . In the regime of negative shear ($C_\Omega < 0$), all solutions found were oscillatory.

We calculate the frequency ω of oscillatory solutions as in the previous section and show the results in Fig. 8. It can be seen that for positive shear, ω approaches 0 as $C_\Omega \rightarrow 33.55$. There also exists a jump in frequency around $C_\Omega \sim 70$, corresponding to a change in the symmetry of the azimuthal field. This is demonstrated in Fig. 9 where time-latitude diagrams of the azimuthal magnetic fields are shown for a representative selection of C_Ω values for models with $\theta_0 = 1^\circ$. The symmetry change corresponding to the frequency jump in Fig. 8 can be seen in the change from antisymmetric about the equator (Fig. 9c, $C_\Omega = 40$) to symmetric (Fig. 9d, $C_\Omega = 80$). The magnetic field is also symmetric in the oscillatory solution found for $C_\Omega = 0$.

All oscillatory solutions with positive (negative) shear show poleward (equatorward) migration in accordance with the Parker-Yoshimura rule (Parker 1955; Yoshimura 1975), compare Figs. 9c and e, respectively, for representative results. The frequency of the oscillations increases with greater C_Ω in accordance with linear theory of $\alpha\Omega$ dynamos, except that

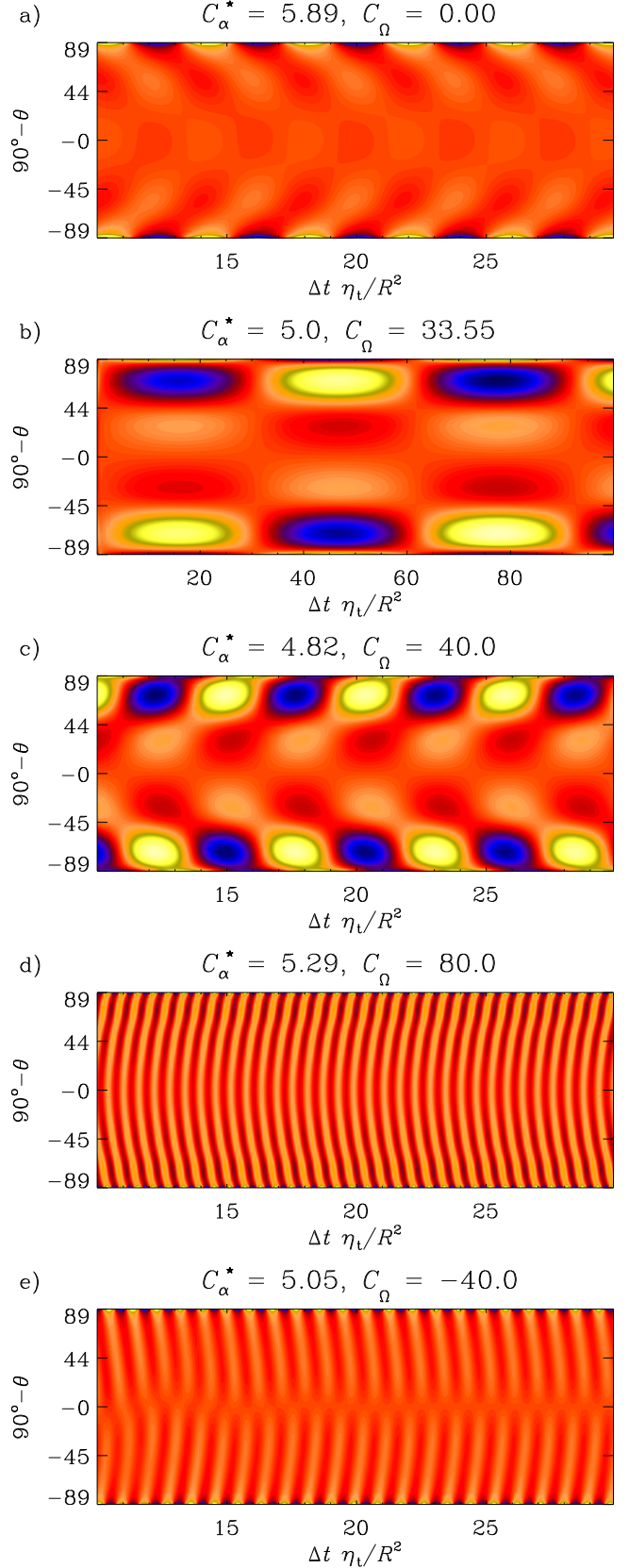


Fig. 9. Azimuthal magnetic field for $\theta_0 = 1^\circ$ with the ASA boundary condition; $\alpha^2\Omega$ dynamo with $\tilde{\mu} = 1$.

there $|\omega| \propto C_\Omega^{1/2}$ (e.g. Brandenburg & Subramanian 2005). Most of the magnetic field is concentrated at high latitudes above

Table 2. C_a^* for runs with $\theta_0 = 0^\circ, 1^\circ, 5^\circ$, and 15° with $a = (1, 0, 0)$ and $e = (1, 0, 0)$ and $\tilde{\mu} = 1$.

θ_0	Boundary condition	C_Ω	C_a^*
0	SAA	60	5.17
1	ASA	60	4.71
5	ASA	60	4.18
15	ASA	60	4.22

$|90^\circ - \theta| > 60^\circ$ for cases where C_Ω is positive, Figs. 9b–d. When $C_\Omega \leq 0$, the field is even more concentrated close to boundaries; see Fig. 9e.

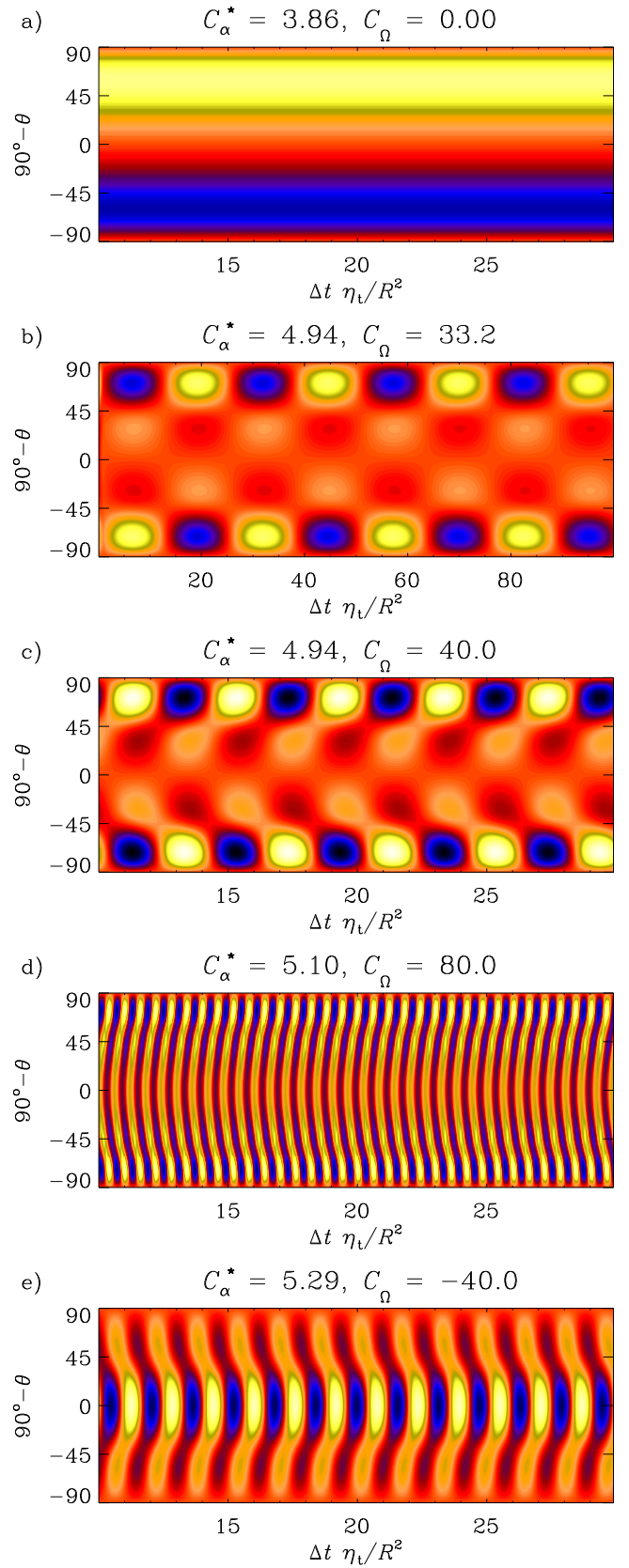
3.2.2. Comparison between $\theta_0 = 0^\circ$ and $\theta_0 = 1^\circ$ cases

The model is now extended to the poles to study the differences between wedges and full spheres. The boundary condition on $\theta_0 = 0^\circ$ is changed to comply with the regularity requirement (SAA). We focus on the case where $\tilde{\mu} = 1$. We consider a few models with $\tilde{\mu} = 0$ and 2 to probe whether the behaviour is similar to the $\theta_0 = 1^\circ$ case. We find that the values of C_a^* are fairly close to those obtained for the corresponding $\theta_0 = 1^\circ$ models; see Fig. 7. Similarly as in the $\theta_0 = 1^\circ$ case, a bifurcation into stationary and oscillatory solutions exists in the positive C_Ω regime with a cut-off point at $C_\Omega \approx 33.2$, which is slightly lower than in the $\theta_0 = 1^\circ$ case. For negative shear, unlike for $\theta_0 = 1^\circ$ where all values produce oscillatory dynamos, the regime for oscillations is found only for $C_\Omega \lesssim -21$. The oscillatory mode gradually disappears and only a stationary mode persists.

The oscillation frequencies (Fig. 8) are similar to those in the case of positive shear. Similarly to the $\theta_0 = 1^\circ$ case, a jump in frequency is observed when the azimuthal field changes symmetry with respect to the equator, as shown in Figs. 10c and d for antisymmetric ($C_\Omega = 40$) and symmetric ($C_\Omega = 80$) field configurations. In the antisymmetric regime, the azimuthal field is concentrated at approximately the same latitudes as for the case $\theta_0 = 1^\circ$. In the symmetric regime where $C_\Omega \gtrsim 70$, the azimuthal field extends to lower latitudes, $|90^\circ - \theta| > 30^\circ$; see Fig. 10d. The main difference occurs at the boundary itself such that for $\theta_0 = 1^\circ$ (ASA) the magnetic field peaks at the boundary whereas it vanishes at the pole for $\theta_0 = 0^\circ$ (SAA). When shear is negative, the field instead becomes concentrated and symmetric around the equator, and in accordance with the Parker-Yoshimura rule, the dynamo has an equatorward drift. The case of negative shear results in a dramatically different concentration of the azimuthal field when compared with the $\theta_0 = 1^\circ$ counterpart; see Figs. 9e and 10e for runs with $C_\Omega = -40$ for the two cases. Even though the values for C_a^* are similar for $\theta_0 = 0^\circ$ and 1° , the frequency of oscillations is less by about a factor of two in the former case; see Fig. 8.

Finally, we examine the effect that θ_0 has on the results by holding C_Ω constant and determining C_a^* . The results are given in Table 2. We find that there is a dependency on θ_0 , but the behaviour is consistent if one goes to the poles and changes the boundary condition; see Table 2 where the change between $\theta_0 = 5^\circ$ and 1° is comparable to the difference between 1° and 0° . All solutions are oscillatory with poleward migration.

Our results suggest that, at least in the cases where $C_\Omega > 0$, a setup with $\theta_0 = 1^\circ$ and the perfect conductor boundary condition (ASA) gives similar results as full sphere models with $\theta_0 = 0^\circ$ and the regularity (SAA) condition. Furthermore, solutions for

**Fig. 10.** Azimuthal magnetic field for $\theta_0 = 0^\circ$ with the SAA boundary condition; $\alpha^2\Omega$ dynamo with $\tilde{\mu} = 1$.

$33.4 < C_\Omega < 75$ are also fairly similar. This indicates that the wedges are a fair approximation of full spheres in this parameter

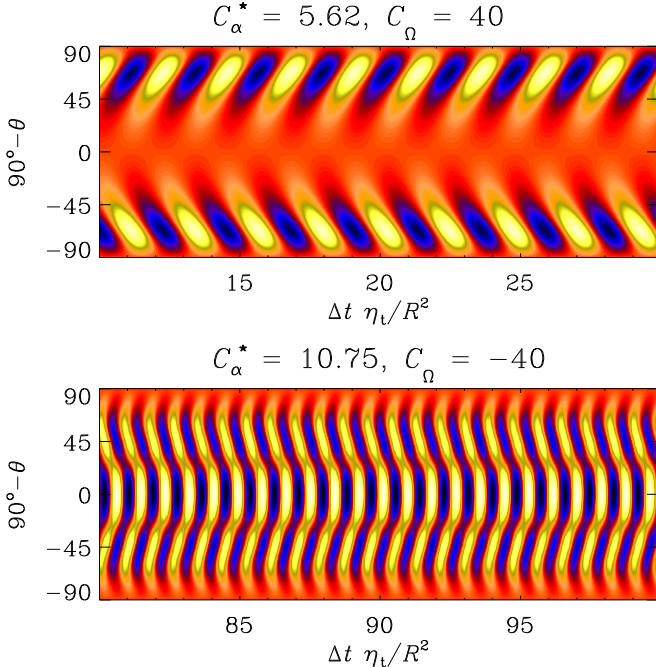


Fig. 11. Azimuthal magnetic field for $\theta_0 = 0^\circ$ with $e_0 = 0.05$, $\tilde{\mu} = 1$, and $\mathbf{a} = \mathbf{e} = (0, 0, 1)$ for $C_\Omega = 40$ (upper panel), and $C_\Omega = -40$ (lower panel).

regime. If the shear is negative, there is a qualitative change in the results between $\theta_0 = 1^\circ$ and $\theta_0 = 0^\circ$ cases. It appears that for weak negative shear, oscillatory solutions are obtained only for the ASA boundary condition.

3.2.3. Varying the α and η_t profiles

Finally, we consider changes to the turbulent magnetic diffusivity profile. We do not perform a thorough parameter study but consider a pair of cases corresponding to $C_\Omega = \pm 40$, $\mathbf{a} = \mathbf{e} = (0, 0, 1)$, $e_0 = 0.05$, $\tilde{\mu} = 1$, and $\theta_0 = 0^\circ$ with regularity conditions for the magnetic field. We show the time–latitude diagrams of the azimuthal field from these models in Fig. 11.

In the case of positive shear, the combination of shear, α and η_t profiles, creates a steady migration poleward at latitudes above $\pm 45^\circ$. Comparing this to an α^2 dynamo with the same profiles of α and η_t (Fig. 4c), and to an $\alpha^2\Omega$ run with no $\sin^{2n}\theta$ contributions in the profiles but the same value of C_Ω (Fig. 10c), shows that the migration direction is reversed in comparison to the α^2 run and that the poleward drift is more coherent than in the $\alpha^2\Omega$ model. These results indicate that the shear determines the direction of the dynamo wave in this parameter regime. The azimuthal field in both of the comparison cases is antisymmetric, and this result also carries over to the case when shear is included with the same α and η_t profiles. The frequency of the oscillations is $\omega = 5.54$, and the critical dynamo parameter is $C_\alpha^* = 5.62$. These values are somewhat close to the values ($\omega = 3.90$ and $C_\alpha^* = 4.94$) obtained in Sect. 3.2.1 in the case with more uniform profiles of the turbulent transport coefficients.

We found earlier that in the case of negative shear, the azimuthal field was symmetric about the equator; see Fig. 10e. With more equatorially concentrated turbulent diffusivity and α profiles we also find solutions with equatorial symmetry, see the bottom panel of Fig. 11. Furthermore, the magnetic field now has a minimum around latitudes $\pm 25^\circ$. The Parker-Yoshimura rule still holds true, and the migration is equatorward. However,

C_α^* has almost doubled from 5.62 to 10.75, and the frequency of oscillations is much larger, $\omega = 14.56$ in comparison to 5.54. The main effect from the more concentrated profiles for α and η_t in the case of $\alpha^2\Omega$ dynamos is seen in the latitudinal profile of the resulting magnetic fields, but the qualitative character of the solutions remains unchanged in comparison to models with simpler latitude dependence of the turbulent transport coefficients.

Concerning the earlier work of Jennings et al. (1990), we can now conclude that they have been lucky, because in their case, although they used negative shear, they found similar solution in a wedge and a full spherical shell. This could have been because in their case $\theta_0 = 45^\circ$. As we now know, the solutions for $\theta_0 = 0^\circ$ and 1° are quantitatively different, although qualitatively similar; see Fig. 8.

4. Conclusions

Motivated by earlier results of global simulations in wedge geometry, we have studied the robustness of oscillatory solutions in α^2 dynamos in simple one-dimensional mean-field dynamo models. We found that the latitudinal boundary conditions play a major role in the realised solutions for α^2 dynamos with a simple $\cos\theta$ profile for α and constant turbulent diffusivity. Imposing the perfect conductor boundary condition creates oscillating solutions only for cases where $\theta_0 \gtrsim 1^\circ$. For $\theta_0 = 1^\circ$, both oscillatory and stationary solutions were found to appear with slightly differing critical dynamo numbers. We found no oscillatory solutions for the normal field (SAS) or regularity conditions (SAA). On the one hand, this motivates future experiments with SAS or SAA conditions in global simulations in wedge geometry. On the other hand, the oscillatory solutions found in global simulations in wedge geometry might still be physical and not an artefact of using a perfect conductor boundary condition on the latitudinal boundaries. Some global simulations in wedge geometry with the SAS condition have already been performed (Käpylä et al. 2016b), but their cases were in a regime where no oscillations occur.

Keeping a simple $\cos\theta$ profile for the α effect and varying the η_t profile creates oscillating solutions with a low frequency and no clear migration or stationary solutions, depending on the value of the underlying (constant) magnetic diffusivity. The magnetic field is largely concentrated near the poles. If the α profile is changed to be concentrated near the equator, similar to profiles observed in rapidly rotating turbulent convection, the magnetic field becomes more evenly distributed towards the equator. The magnetic field also exhibits clear equatorward migration and antisymmetry with respect to the equator. The overall conclusion is that α^2 dynamos can produce solar-like magnetic activity if the α effect and turbulent diffusivity have latitudinal profiles that are sufficiently concentrated toward the equator. One may speculate that this could actually be the case in the spherical wedge simulations of Käpylä et al. (2012), where most of the magnetic activity and most of the magnetic helicity were found to occur away from the axis, outside the inner tangent cylinder.

We then added positive shear to study $\alpha^2\Omega$ dynamos and how they connect to the pure α^2 solutions in the same wedge geometry with $\theta_0 = 1^\circ$. For weak shear the azimuthal magnetic field is concentrated at the poles and shifts equatorward. Over a certain interval in C_Ω , which depends on the added local friction $\tilde{\mu}$, oscillatory solutions are found and the field is more concentrated across all upper latitudes. For $\tilde{\mu} = 1$, we found that both stationary and oscillatory solutions exist with the oscillatory one having a substantially higher critical dynamo number. Going to a full sphere with $\theta_0 = 0^\circ$ and changing the boundary condition

to SAA produced qualitatively and quantitatively similar results when the shear was positive. Results are less similar if negative shear is introduced. When $\theta_0 = 1^\circ$, all solutions with $C_\Omega < 0$ were found to oscillate. However, when $\theta_0 = 0^\circ$, shear had to exceed a critical value, $C_\Omega < -21$, for solutions to oscillate. Furthermore, the structure of the azimuthal field over time was significantly different, showing symmetry about the equator and concentration at the equator. In all cases with shear, the Parker-Yoshimura rule was found to be obeyed where oscillatory solutions with negative shear migrated equatorward and positive shear, poleward. When combining the η_t profile with shear, the direction of migration was determined by the sign of C_Ω . The frequency increased in the case of negative shear when using an η_t and α profile with higher order terms.

In summary, we may conclude that large-scale dynamo action in spherical domains can, under certain conditions, be approximated by solutions in wedge-shaped geometries. This may well be the case for the simulations of Käpylä et al. (2012, 2016a). At least in the outer parts, close to the surface, those solutions exhibit a phase relation between poloidal and toroidal fields that is only seen in α^2 dynamos of the type presented in Sect. 3.1; see Sect. 3.6 of Käpylä et al. (2013b). A subsequent study by Warnecke et al. (2014) showed, however, that the equatorward migration is the result of a standard $\alpha^2\Omega$ dynamo operating in deeper layers; see their Figs. 5c and d.

The angular velocities used in the simulations of Käpylä et al. (2013b) were probably too large to represent the Sun. The solar dynamo may therefore still be of α^2 type. However, as we have seen, those dynamos would only be oscillatory if the polar regions can be regarded as highly conducting; see Sect. 3.1.1. There may be alternative possibilities for obtaining oscillatory solutions to the α^2 dynamo. One possibility is to study the effect of decreasing the (microphysical) magnetic diffusivity even further. Another possibility is to study the memory effect, which has recently been identified as a means to facilitate oscillatory behaviour (Rheinhardt & Brandenburg 2012), although so far only decaying solutions have been found to be modified in that way (Devlen et al. 2013). However, under suitable conditions such solutions can indeed become oscillatory (Rheinhardt et al. 2014) and may present a possible solution to the problem where equatorward motion obtained via varying the α profile with $a = (0, 0, 1)$, for example, is limited to certain latitudes.

Acknowledgements. The authors thank Nordita for hospitality during their visits. Financial support from the Vilho, Yrjö and Kalle Väisälä Foundation (EC), the Academy of Finland grants No. 136189, 140970 (P.J.K.) and the Academy of Finland Centre of Excellence ReSoLVE (272157; M.J.K. and P.J.K.), as well as the Swedish Research Council grants 621-2011-5076 and 2012-5797, and the European Research Council under the AstroDyn Research Project 227952 are acknowledged. We acknowledge CSC – IT Center for Science Ltd., who are administered by the Finnish Ministry of Education, for the allocation of computational resources.

References

- Augustson, K., Brun, A. S., Miesch, M. S., & Toomre, J. 2015, *ApJ*, **809**, 149
 Babcock, H. W. 1961, *ApJ*, **133**, 572
 Brandenburg, A., & Subramanian, K. 2005, *Phys. Rev.*, **417**, 1
 Brandenburg, A., Krause, F., Meinel, R., Moss, D., & Tuominen, I. 1989, *MNRAS*, **213**, 411
 Brandenburg, A., Nordlund, Å., Stein, R. F., & Torkelsson, U. 1995, *A&A*, **446**, 741
 Brandenburg, A., Candelaresi, S., & Chatterjee, P. 2009, *ApJ*, **398**, 1414
 Brown, B. P., Browning, M. K., Brun, A. S., Miesch, M. S., & Toomre, J. 2010, *ApJ*, **711**, 424
 Candelaresi, S., Hubbard, A., Brandenburg, A., & Mitra, D. 2011, *Phys. Plasmas*, **18**, 012903
 Cattaneo, F., & Hughes, D. W. 2006, *J. Fluid. Mech.*, **553**, 401
 Choudhuri, A. R., Schüssler, M., & Dikpati, M. 1995, *A&A*, **303**, L29
 Devlen, E., Brandenburg, A., & Mitra, D. 2013, *MNRAS*, **432**, 1651
 Duarte, L. D. V., Wicht, J., Browning, M. K., & Gastine, T. 2016, *MNRAS*, **456**, 1708
 Jennings, R., Brandenburg, A., Moss, D., & Tuominen, I. 1990, *A&A*, **230**, 463
 Jiang, J., & Wang, J.-X. 2006, *Chin. J. Astron. Astrophys.*, **2**, 227
 Käpylä, P. J., Korpi, M. J., Ossendrijver, M., & Stix, M. 2006, *A&A*, **455**, 401
 Käpylä, P. J., Korpi, M. J., & Brandenburg, A. 2009, *A&A*, **500**, 633
 Käpylä, P. J., Mantere, M. J., Guerrero, G., Brandenburg, A., & Chatterjee, P. 2011, *A&A*, **531**, A162
 Käpylä, P. J., Mantere, M. J., & Brandenburg, A. 2012, *ApJ*, **755**, L22
 Käpylä, P. J., Mantere, M. J., & Brandenburg, A. 2013a, *Geophys. Astrophys. Fluid Dyn.*, **107**, 244
 Käpylä, P. J., Mantere, M. J., Cole, E., Warnecke, J., & Brandenburg, A. 2013b, *ApJ*, **778**, 41
 Käpylä, M. J., Käpylä, P. J., Olspert, N., et al. 2016a, *A&A*, **589**, A56
 Käpylä, P. J., Käpylä, M. J., Olspert, N., Warnecke, J., & Brandenburg, A. 2016b, *A&A*, submitted [[arXiv:1605.05885](https://arxiv.org/abs/1605.05885)]
 Kitchatinov, L. L., Rüdiger, G., & Pipin, V. V. 1994, *Astron. Nachr.*, **315**, 157
 Kuzanyan, K. M., & Sokoloff, D. D. 1995, *Geophys. Astrophys. Fluid Dyn.*, **81**, 113
 Masada, Y., & Sano, T. 2014, *ApJ*, **794**, L6
 Miesch, M. S., Elliott, J. R., Toomre, J., et al. 2000, *ApJ*, **532**, 593
 Mitra, D., Tavakol, R., Käpylä, P. J., & Brandenburg, A. 2010, *ApJ*, **719**, L1
 Moss, D., Sokoloff, D., Kuzanyan, K., & Petrov, A. 2004, *Geophys. Astrophys. Fluid Dyn.*, **98**, 257
 Parker, E. N. 1955, *ApJ*, **122**, 293
 Rädler, K.-H. 1980, *ApJ*, **301**, 101
 Rheinhardt, M., & Brandenburg, A. 2012, *Astron. Nachr.*, **333**, 71
 Rheinhardt, M., Devlen, E., Rädler, K.-H., & Brandenburg, A. 2014, *MNRAS*, **441**, 116
 Rüdiger, G., & Brandenburg, A. 1995, *A&A*, **296**, 557
 Rüdiger, G., Elstner, D., & Ossendrijver, M. 2003, *A&A*, **406**, 15
 Steenbeck, M., & Krause, F. 1969a, *Astron. Nachr.*, **291**, 49
 Steenbeck, M., & Krause, F. 1969b, *Astron. Nachr.*, **291**, 271
 Steenbeck, M., Krause, F., & Rädler, K.-H. 1966, *Z. Naturforsch. A*, **21**, 369
 Sur, S., Brandenburg, A., & Subramanian, K. 2008, *MNRAS*, **385**, L15
 Ulrich, R. K., & Boyden, J. E. 2005, *ApJ*, **620**, L123
 Warnecke, J., Käpylä, P. J., Mantere, M. J., & Brandenburg, A. 2013, *ApJ*, **778**, 141
 Warnecke, J., Käpylä, P. J., Käpylä, M. J., & Brandenburg, A. 2014, *ApJ*, **796**, L12
 Warnecke, J., Rheinhardt, M., Käpylä, P. J., Käpylä, M. J., & Brandenburg, A. 2016, *A&A*, submitted [[arXiv:1601.03730](https://arxiv.org/abs/1601.03730)]
 Yoshimura, H. 1975, *ApJ*, **201**, 740